Hydrocarbons

Deutsche Ausgabe: DOI: 10.1002/ange.201507573
Internationale Ausgabe: DOI: 10.1002/anie.201507573

Dipolar Quinoidal Acene Analogues as Stable Isoelectronic Structures of Pentacene and Nonacene

*Xueliang Shi, Weixiang Kueh, Bin Zheng, Kuo-Wei Huang, and Chunyan Chi**

Abstract: *Quinoidal thia-acene analogues, as the respective isoelectronic structures of pentacene and nonacene, were synthesized and an unusual 1,2-sulfur migration was observed during the Friedel–Crafts alkylation reaction. The analogues display a closed-shell quinoidal structure in the ground state with a distinctive dipolar character. In contrast to their acene isoelectronic structures, both compounds are stable because of the existence of more aromatic sextet rings, a dipolar character, and kinetic blocking. They exhibit unique packing in single crystals resulting from balanced dipole–dipole and [C–H···π]/[C–H···S] interactions.*

Functionalized acenes/heteroacenes have been demonstrated to be good active materials in organic electronics.[1] However, the lack of efficient synthetic methods and the unstable nature of longer acenes/heteroacenes limit their potential applications. Typical decomposition pathways of longer acenes/heteroacenes involve: 1) addition with singlet oxygen to form an endoperoxide[2] and further oxidation to the corresponding quinone;[3] 2) Diels–Alder reaction with dienophiles (e.g. alkyne substituents) or [4+4] cycloaddition of the acene backbone.[4] In addition, the solubility issue should be also addressed to obtain characterizable and processible materials. Chemists have developed various strategies to stabilize and solubilize acenes/heteroacenes including: 1) substitution with bulky aryl and silylethynyl groups;[5] 2) substitution with electron-deficient carboximide, fluorine and cyano groups;[6] 3) incorporation of imine-type nitrogen atoms to the backbone;[7] and 4) annulation of cyclopenta-moieties along the zig-zag edges.[8]

Our group has a longstanding interest in acenes/heteroacenes chemistry,[9] and recently we developed a new type of quinoidally conjugated dithia-acene analogue (e.g., 5,12-dithiapentacene; Figure 1) which displayed remarkable stability and distinctive electronic properties.[10] The switching from a *cis*-1,3-butadiene conjugation to a quinoidal conjugation eliminates the possible cycloaddition reactions and at the same time increases the benzenoid character by releasing one additional aromatic sextet ring (highlighted in blue in Figure 1), and thus improves the stability and dramatically changes the ground-state electronic structure. We believe that this concept can be further extended to longer acenes such as highly reactive nonacene which was predicted to have an open-shell singlet diradical ground state (Figure 1).[11] However, by counting two lone-pair electrons for each sulfur atom, these quinoidal dithia-acenes possess two more π electrons than the corresponding acene derivatives (e.g., 24 πe for 5,12-dithiapentacene while 22 πe for pentacene; Figure 1). Hence, we became interested in a new type of quinoidal acene analogues such as **A**–**C** (Figure 1) by removing one sulfur atom (thus 2 πe) per *p*-quinodimethane (*p*-QDM) unit and the obtained structures now can be regarded as the isoelectronic structures of the respective acenes (Figure 1). They are better described as "acene-like molecules" rather than "acenes" because of existence of more than one aromatic sextet rings. Besides the closed-shell quinoidal structure, one open-shell diradical resonance form and one dipolar zwitter-

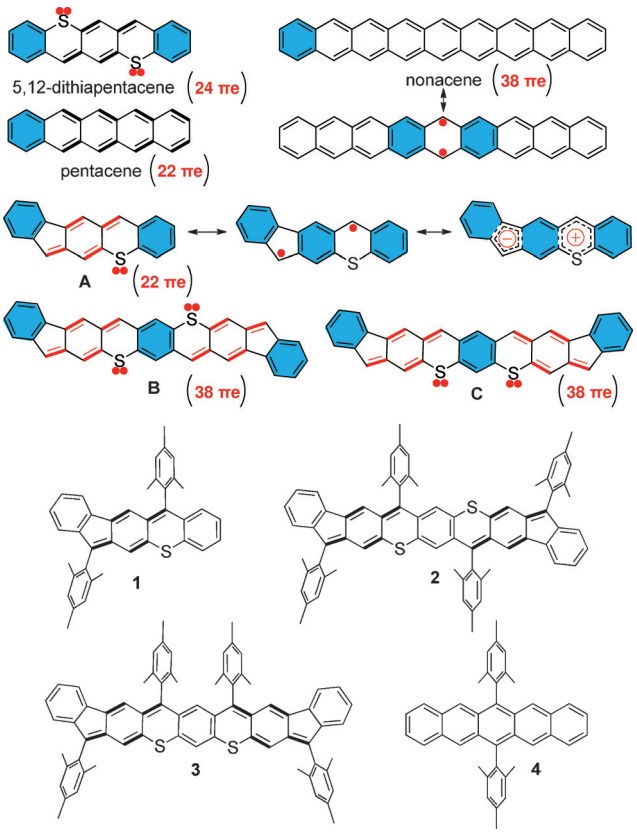

Figure 1. Structures of 5,12-dithiapentacene, pentacene, nonacene, and their quinoidal thia-acene isoelectronic structures.

[*] X. Shi, W. Kueh, Prof. C. Chi
Department of Chemistry, National University of Singapore
3 Science Drive 3, 117543 (Singapore)
E-mail: chmcc@nus.edu.sg
Dr. B. Zheng, Prof. K.-W. Huang
KAUST Catalysis Center and Division of Physical Sciences & Engineering, King Abdullah University of Science and Technology (KAUST), Thuwal 23955-6900 (Saudi Arabia)

Supporting information for this article is available on the WWW under http://dx.doi.org/10.1002/anie.201507573.

ionic resonance form are also supposed to contribute to the ground-state structure because of the recovery of one more aromatic sextet ring in the latter two forms (Figure 1). In this context, we started to investigate the chemistry, structure, and physical properties of the derivatives of **A** (isoelectronic pentacene) and **B** (isoelectronic nonacene), **1** and **2**, respectively, and compare them with the corresponding acenes such as **4** and reported nonacene derivatives.[2b] Bulky mesityl substituents are attached at the methylene site of the *p*-QDM moiety to stabilze the possible diradical structure. However, instead of the target compound **2**, an isomer **3** was obtained through an unusual 1,2-sulfur migration process, and it also serves as a good isoelectronic structure of nonacene.

The syntheses of **1**–**3** were based on an intramolecular Friedel–Crafts-alkylation/dehydrogenation strategy (Scheme 1). Suzuki coupling between the dibromo diketone **5** (see the Supporting Information) and one equivalent of the phenylboronic acid gave the key intermediate **6**, and subsequent nucleophilic substitution with thiophenol in the presence of CuI and K_2CO_3 afforded the asymmetric diketone **7**. Reduction of **7** gave the diol **8** and subsequent $BF_3{\cdot}Et_2O$-mediated Friedel–Crafts alkylation generated the dihydro compound **9**. Finally the target product **1** was obtained by oxidative dehydrogenation with *p*-chloranil in refluxing toluene. Following a similar protocol, reaction between **6** and benzene-1,4-dithiol failed to give the desired tetraketone **10**. Alternatively, palladium-catalyzed C–S coupling afforded **10** in 65% yield. After a similar reduction/Friedel–Crafts alkylation/dehydrogenation sequence from **10**, surprisingly, the *meta*-dithia isomer **3**, instead of the *para*-dithia compound **2**, was obtained in 50% yield over three steps, as confirmed by X-ray crystallographic analysis. The structure of **10** was also identified by X-ray crystallographic analysis.[12] The rearrangement reaction likely does not happen during either the reduction (with $LiAlH_4$) or oxidative dehydrogenation (with *p*-chloranil) steps. Therefore, the formation of the *meta*-dithia compound is likely due to 1,2-sulfur migration via a spirocyclic cationic intermediate during the ring cyclization reaction in the presence of $BF_3{\cdot}Et_2O$ (Scheme 1).[13] However, the main driving force for this particular migration and the reason for the exclusive generation of **3**, rather than the proposed **2**, are not clear at this stage. For comparison, the 6,13-dimesityl pentacene **4** was synthesized according to a published procedure with minor modification (see the Supporting Information).[3a]

The compounds **1** and **3** are extremely stable in air, and is in contrast to their corresponding reactive pentacene (such as **4**) and nonacene derivatives.[2b] The compound **1** displays distinctly different absorption spectrum from that of **4** in dichloromethane, with an intense absorption band at $\lambda =$ 360 nm and a broad band at $\lambda = 650$–900 nm (Figure 2a). Time-dependent density functional theory (TD DFT) calculations (B3LYP/6-31G*; see the Supporting Information) indicated that the longest-wavelength absorption band originates from HOMO→LUMO transition ($\lambda_{max} = 677.7$ nm, oscillator strength $f = 0.1940$; see Table S1 and Figure S2 in the Supporting Information). In contrast, the pentacene derivative **4** shows a well-resolved p-band with a maximum at $\lambda = 601$ nm. The compound **3** exhibits a similar band structure to that of **1**, but both bands are red-shifted (by 44 nm for the longest absorption band), consistent with an extension of π-electron delocalization, and in agreement with the TD DFT calculations ($\lambda_{max} = 728.6$ nm, $f = 0.9865$; see Table S2 and Figure S2). The corresponding nonacene derivatives show a weak *p*-band with an absorption maximum shifted beyond $\lambda = 1000$ nm.[2b] Such a dramatic difference between the acenes and our acene-like molecules can be explained by the existence of more aromatic sextet rings in our new quinoidal systems, which increase the energy gap. The optical energy gap (E_g^{opt}) was determined as 1.34, 1.28, 2.02, and 1.20 eV for **1**, **3**, **4**, and Anthony's nonacene derivatitve, respectively, from the onset of the lowest-energy absorption. It was hypothesized that the long-wavelength broad absorption band is attributed to the intramolecular charge transfer

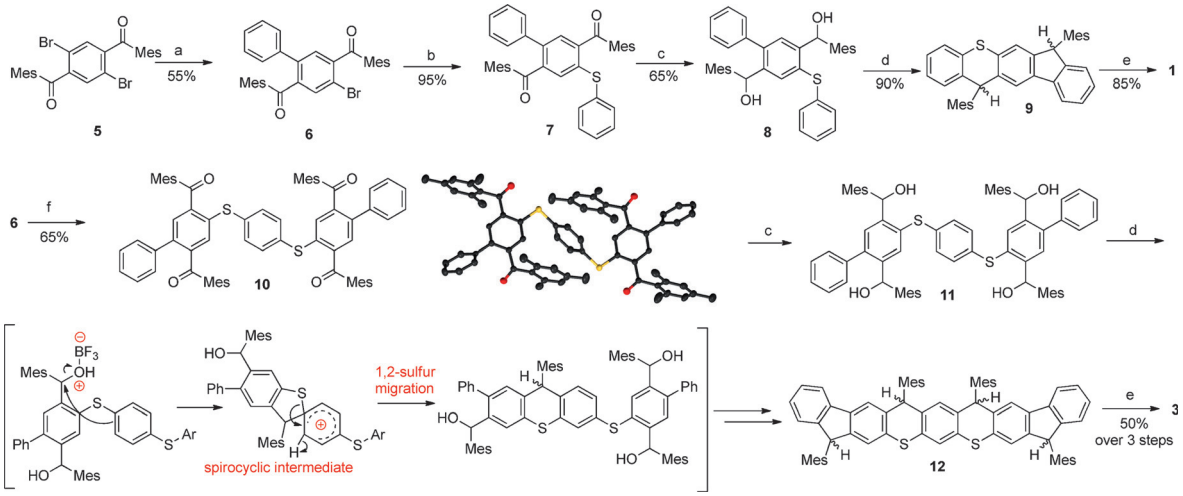

Scheme 1. Reagents and conditions: a) phenylboronic acid, $[Pd(PPh_3)_4]$, Na_2CO_3, toluene/water (5:1), 100 °C, overnight; b) thiophenol, CuI, K_2CO_3, DMF, 100 °C, overnight; c) $LiAlH_4$, anhydrous THF, for **8**: 0 °C to RT, overnight; for **11**: 0 °C to RT. −50 °C overnight; d) $BF_3{\cdot}Et_2O$, anhydrous CH_2Cl_2, 0 °C to RT, 3 h; e) *p*-chloranil, toluene, reflux, 5 days; f) benzene-1,4-dithiol, $[Pd_2(dba)_3]$, dppf, iPr_2NEt, DMF, 100 °C, overnight. dba = dibenzylideneacetone, DMF = *N*,*N*-dimethylformamide, dppf = 1,1′-bis(diphenylphosphino)ferrocene, Mes = mesityl, THF = tetrahydrofuran.

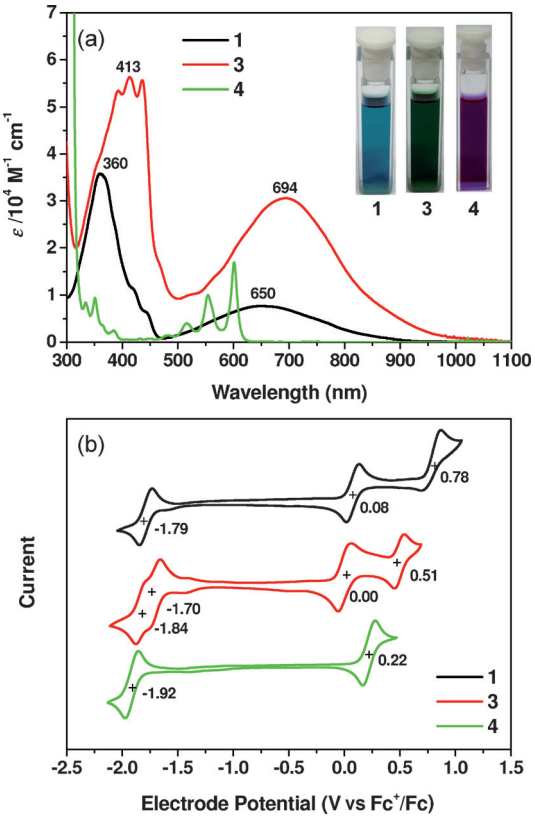

Figure 2. a) UV-vis-NIR absorption spectra of **1**, **3**, and **4** recorded in CH_2Cl_2. b) Cyclic voltammograms of **1**, **3**, and **4** in CH_2Cl_2 with 0.1 M Bu_4NPF_6 as supporting electrolyte, Ag/AgCl as reference electrode, Pt wire as counter electrode, and scan rate at 50 mVs^{-1}. Fc = ferrocene. The electrode potential was externally calibrated by Fc^+/Fc couple.

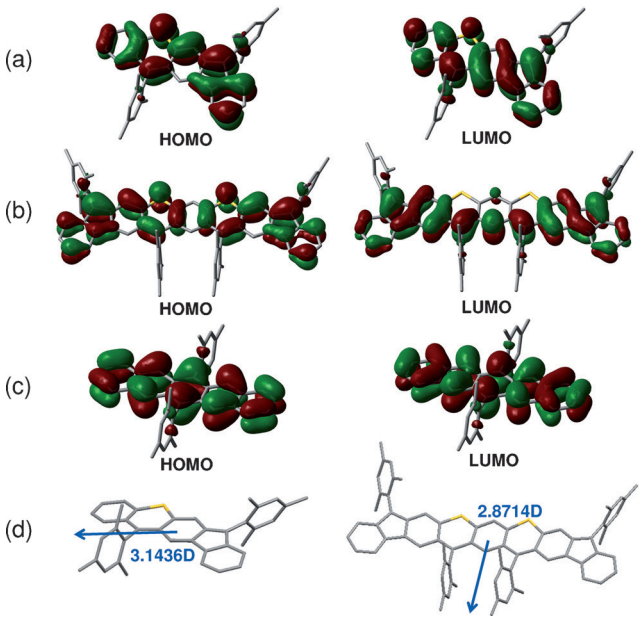

Figure 3. Calculated (B3LYP/6-31G*) frontier molecular orbital profiles and energy levels of **1** (a), **3** (b), and **4** (c), and the dipoles of **1** and **3** (d).

(ICT) and thus the absorption spectra of **1** and **3** have been studied in different solvents (see Figure S3). However, it is found that the positions of the absorption peak for both compounds are almost independent of solvent polarity, thus indicating that there are only weak ICTs in this system. No emission can be observed from either **1** or **3**. The HOMO and LUMO profiles of **1** and **3** indeed show some disjointed characters compared to that of **4**, thus resulting in a significant dipole moment of 3.1436 D and 2.8714 D, respectively (Figure 3). The broadened and red-shifted absorption bands in **1** and **3** are thus better ascribed to a weak intramolecular donor–acceptor interaction in a quinoidally conjugated skeleton.

The compounds **1** and **3** display excellent amphoteric redox behavior with one or two reversible reduction waves (half-wave potential $E_{1/2}^{red} = -1.79$ for **1** and -1.84, -1.70 V for **3**, *vs* Fc^+/Fc) and two reversible oxidation waves (half-wave potential $E_{1/2}^{ox} = -0.08$, 0.78 V for **1** and 0.00, 0.51 V for **3**; Figure 2b). For comparison, **4** exhibits one reversible oxidation wave ($E_{1/2}^{ox} = 0.22$ V) and one reversible reduction wave ($E_{1/2}^{red} = -1.92$ V). The HOMO and LUMO energy levels were estimated to be -4.79 (**1**), -4.72 (**3**), -4.94 eV (**4**), and -3.10 (**1**), -3.20 (**3**), -2.96 eV (**4**), respectively. The electrochemical energy gap (E_g^{EC}) was thus determined to be 1.69, 1.52, and 1.98 eV for **1**, **3**, and **4**, respectively. The high-lying HOMO energy levels allow us to access the radical cations of **1**, **3**, and **4** by oxidative titration with $SbCl_5$ in CH_2Cl_2, and characteristic absorption bands at $\lambda = 419$, 638, 974 nm for $\mathbf{1}^{+\cdot}$, $\lambda = 453$, 835, 1071, 1224 nm for $\mathbf{3}^{+\cdot}$, and $\lambda = 430$, 835, 943, 1195 nm for $\mathbf{4}^{+\cdot}$, were observed (see Figure S4).

Single crystals of **1**, **3**, and **4**, suitable for X-ray crystallography analysis, were successfully grown and analyzed. The ORTEP drawings and three-dimensional (3D) packing structures are shown in Figure 4.[14] The solid-state packing of **1** is highly symmetric (tetragonal; space group $I4_1/a$), even though the molecule itself is asymmetric. The backbone of **1** is essentially planar, with the two mesityl groups oriented almost perpendicularly to the backbone. This orientation disrupts the regular π stacking or herringbone arrangements observed in common acenes/heteroacenes derivatives. Alternatively, molecules of **1** are packed into a squarelike tetrameric structure through intermolecular dipole–dipole interactions and [C-H···π] interactions (2.692/2.895 Å) between the methyl groups of one molecule to the π backbone of another molecule. Such tetrameric structures are further packed into a highly symmetric 3D structure through dipole–dipole interactions. No close [S···S] interaction was observed. In comparison, **3** crystalizes in a triclinic lattice system, with space group P1. One toluene molecule per molecule is incorporated into the crystal lattice. The backbone of **3** is slightly distorted, with the four mesityl rings oriented almost perpendicularly to the backbone. Interestingly, **3** packs in a slipped face-to-face manner mainly through [C–H···S] interactions (2.895/2.994 Å) between one methyl group in one molecule with sulfur atom in the neighboring molecule and [C–H···π] interactions (2.744/2.780 Å) between methyl groups of one molecule and the π backbone of another molecule. These interactions suppress the normally observed anti-parallel dipole–dipole interaction in a dipolar molecule and the dipole moments of all molecules in this case point to

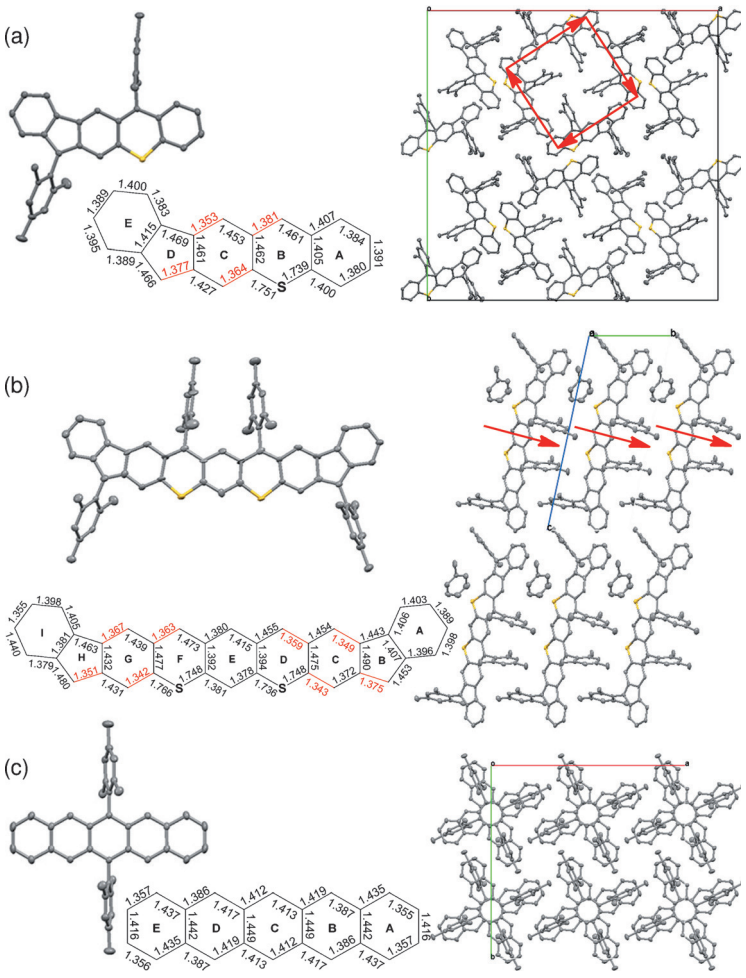

Figure 4. X-ray crystallographic structures and 3D packing of **1** (a), **3** (b) and **4** (c), and bond lengths of the π-conjugated core frameworks. Hydrogen atoms are omitted for clarity. The arrows roughly denote the dipole moments.

the same direction. The compound **4** has a slightly distorted backbone with the mesityl groups nearly perpendicular to the backbone. Because of the bulky substituent, no close π–π interaction was observed. The molecules are packed into a compact structure with tetragonal symmetry, space group $I4_1/a$, mainly through intermolecular [C–H···π] interactions.

As mentioned above, dipolar quinoidal polycyclic hydrocarbons could exhibit unique singlet diradical and zwitterionic character and diminished bond-length alternation (BLA).[15] Hence, bond length analysis was performed to analyze the ground-state geometry of **1** and **3**, in comparison to that of **4** (Figure 4). As observed, the central ring C of **1** displays noticeable BLA, thus indicating a significant quinoidal conjugation. The two terminal rings, A and E, possess relatively constant bond lengths, thus implying their large aromatic character. Similarly, rings C and G of **3** also show large BLA, while the central ring E and the two terminal rings, A and I, possess relatively constant bond lengths. These data confirm that both **1** and **3** have a quinoidal structure in their ground state and have little contribution from the diradical and dipolar zwitterionic resonance forms, which is in good agreement with the UV-vis-NIR absorption spectra in different solvents and DFT calculations. For comparison, the BLA of **4** exhibits a typical diene conjugation motif.

In summary, two quinoidal thia-acene analogues, **1** and **3**, as isoelectronic structures of pentacene and nonacene,respectively, were successfully prepared and an unusual 1,2-sulfur migration was discovered during the synthesis. The ground-state geometry and electronic properties of **1** and **3** were systematically investigated both experimentally and theoretically. The compounds **1** and **3** show excellent solubility and stability and distinctively different absorption spectra compared to their acene counterparts, and can be explained by their unique dipolar quinoidal structure. No typical π stacking or herringbone arrangement is observed in the crystalline form of both compounds because of the bulky mesityl substituents. However, a balance between the dipole–dipole interaction and intermolecular [C–H···π]/[C–H···S] interaction result in unique packing structures in the solid state. All experimental data and theoretical calculations point to the same conclusion, that is, both **1** and **3** have a typically closed-shell quinoidal structure in their ground state with a small diradical or bipolar/zwitterionic character. This work again demonstrates the efficiency of the quinodimethane approach to acenes and will shed light on the synthesis of stable higher-order acene and heteroacene analogues in the future.

Acknowledgements

C.C. acknowledges financial support from the MOE Tier 1 grant (R-143-000-573-112), Tier 2 grant (MOE2014-T2-1-080), and Tier 3 programme (MOE2014-T3-1-004). K.-W.H. acknowledges financial support from KAUST. We thank Dr. Bruno Donnadieu and Dr. Tan Geok Kheng for the crystallographic analysis.

Keywords: aromaticity · density functional calculations · polycyclic aromatic hydrocarbons · structure determination · X-ray diffraction

How to cite: *Angew. Chem. Int. Ed.* **2015**, *54*, 14412–14416
Angew. Chem. **2015**, *127*, 14620–14624

[1] Review articles: a) M. Bendikov, F. Wudl, D. F. Perepichka, *Chem. Rev.* **2004**, *104*, 4891; b) J. E. Anthony, *Chem. Rev.* **2006**, *106*, 5028; c) J. E. Anthony, *Angew. Chem. Int. Ed.* **2008**, *47*, 452; *Angew. Chem.* **2008**, *120*, 460; d) Z. Sun, Q. Ye, C. Chi, J. Wu, *Chem. Soc. Rev.* **2012**, *41*, 7857; e) K. Takimiya, I. Osaka, T. Mori, M. Nakano, *Acc. Chem. Res.* **2014**, *47*, 1493.

[2] a) S. H. Chan, H. K. Lee, Y. M. Wang, N. Y. Fu, X. M. Chen, Z. W. Cai, H. N. C. Wong, *Chem. Commun.* **2005**, 66; b) B. Purushothaman, M. Bruzek, S. R. Parkin, A. F. Miller, J. E. Anthony, *Angew. Chem. Int. Ed.* **2011**, *50*, 7013; *Angew. Chem.* **2011**, *123*, 7151.

[3] a) I. Kaur, W. Jia, R. P. Kopreski, S. Selvarasah, R. Dokmeci, C. Pramanik, N. E. Mcgruer, G. P. Miller, *J. Am. Chem. Soc.* **2008**,

130, 16274; b) B. Kohl, F. Rominger, M. Mastalerz, *Angew. Chem. Int. Ed.* **2015**, *54*, 6051; *Angew. Chem.* **2015**, *127*, 6149.
[4] a) O. Berg, E. L. Chronister, T. Yamashita, G. W. Scott, R. M. Sweet, J. Calabrese, *J. Phys. Chem. A* **1999**, *103*, 2451; b) B. Purushothaman, S. R. Parkin, J. E. Anthony, *Org. Lett.* **2010**, *12*, 2060.
[5] a) J. E. Anthony, D. L. Eaton, S. R. Parkin, *Org. Lett.* **2002**, *4*, 15; b) M. M. Payne, S. R. Parkin, J. E. Anthony, *J. Am. Chem. Soc.* **2005**, *127*, 8028; c) D. Chun, Y. Cheng, F. Wudl, *Angew. Chem. Int. Ed.* **2008**, *47*, 8380; *Angew. Chem.* **2008**, *120*, 8508; d) H. Qu, C. Chi, *Org. Lett.* **2010**, *12*, 3360; e) W. Fudickar, T. Linker, *J. Am. Chem. Soc.* **2012**, *134*, 15071.
[6] a) Y. Sakamoto, T. Suzuki, M. Kobayashi, Y. Gao, Y. Fukai, Y. Inoue, F. Sato, S. Tokito, *J. Am. Chem. Soc.* **2004**, *126*, 8138; b) H. Qu, W. B. Cui, J. Li, J. Shao, C. Chi, *Org. Lett.* **2011**, *13*, 924; c) S. Katsuta, D. Miyagi, H. Yamada, T. Okujima, S. Mori, K. I. Nakayama, H. Uno, *Org. Lett.* **2011**, *13*, 1454; d) S. Katsuta, K. Tanaka, Y. Maruya, S. Mori, S. Masuo, T. Okujima, H. Uno, K.-I. Nakayama, H. Yamada, *Chem. Commun.* **2011**, *47*, 10112.
[7] a) B. Gao, M. Wang, Y. Cheng, L. Wang, X. Jing, F. Wang, *J. Am. Chem. Soc.* **2008**, *130*, 8297; b) U. H. F. Bunz, *Chem. Eur. J.* **2009**, *15*, 6780; c) U. H. F. Bunz, J. U. Engelhart, B. D. Lindner, M. Schaffroth, *Angew. Chem. Int. Ed.* **2013**, *52*, 3810; *Angew. Chem.* **2013**, *125*, 3898; d) U. H. F. Bunz, *Acc. Chem. Res.* **2015**, *48*, 1676.
[8] a) J. D. Wood, J. L. Jellison, A. D. Finke, L. Wang, K. N. Plunkett, *J. Am. Chem. Soc.* **2012**, *134*, 15783; b) A. N. Lakshminarayana, J. Chang, J. Luo, B. Zheng, K.-W. Huang, C. Chi, *Chem. Commun.* **2015**, *51*, 3604.
[9] a) H. Qu, C. Chi, *Curr. Org. Chem.* **2010**, *14*, 2070; b) Q. Ye, C. Chi, *Chem. Mater.* **2014**, *26*, 4046.
[10] Q. Ye, J. Chang, X. Shi, G. Dai, W. Zhang, K.-W. Huang, C. Chi, *Org. Lett.* **2014**, *16*, 3966.
[11] a) M. Bendikov, H. M. Duong, K. Starkey, K. N. Houk, E. A. Carter, F. Wudl, *J. Am. Chem. Soc.* **2004**, *126*, 7416; b) C. Tönshoff, H. F. Bettinger, *Angew. Chem. Int. Ed.* **2010**, *49*, 4125; *Angew. Chem.* **2010**, *122*, 4219.
[12] CCDC 1059907 (**10**) contains the supplementary crystallographic data for this paper. These data can be obtained free of charge from The Cambridge Crystallographic Data Centre via www.ccdc.cam.ac.uk/data_request/cif.
[13] a) G. Capozzi, G. Melloni, G. Modena, M. Piscitelli, *Tetrahedron Lett.* **1968**, *9*, 4039; b) G. Capozzi, G. Melloni, G. Modena, *J. Chem. Soc. C* **1970**, 2621; c) G. Capozzi, G. Melloni, G. Modena, *J. Org. Chem.* **1970**, *35*, 1217; d) M. S. Newman, *Acc. Chem. Res.* **1972**, *5*, 354; e) G. Capozzi, G. Melloni, G. Modena, *J. Chem. Soc. Perkin Trans. 1* **1973**, 2250.
[14] CCDC 1059905 (**1**), 1059906 (**3**), and 1408042 (**4**) contain the supplementary crystallographic data for this paper. These data can be obtained free of charge from The Cambridge Crystallographic Data Centre via www.ccdc.cam.ac.uk/data_request/cif.
[15] Review articles: a) Z. Sun, J. Wu, *J. Mater. Chem.* **2012**, *22*, 4151; b) A. Shimizu, Y. Hirao, T. Kubo, M. Nakano, E. Botek, B. Champagne, *AIP Conf. Proc.* **2012**, *1504*, 399; c) Z. Sun, Z. Zeng, J. Wu, *Chem. Asian J.* **2013**, *8*, 2894; d) M. Abe, *Chem. Rev.* **2013**, *113*, 7011; e) Z. Sun, Z. Zeng, J. Wu, *Acc. Chem. Res.* **2014**, *47*, 2582; f) T. Kubo, *Chem. Rec.* **2015**, *15*, 218; g) Z. Zeng, X. Shi, C. Chi, J. T. L. Navarrete, J. Casado, J. Wu, *Chem. Soc. Rev.* **2015**, *44*, 6578.

Received: August 13, 2015
Published online: October 8, 2015